Received: 16 February 2019 | Revised: 14 May 2019 | Accepted: 21 August 2019

DOI: 10.1002/we.2417

WILEY

RESEARCH ARTICLE

Projected changes in wind speed and its energy potential in China using a high-resolution regional climate model

Junhong Guo[1,3] | Guohe Huang[2,3] | Xiuquan Wang[4] | Ye Xu[1,3] | Yongping Li[5]

[1]Key Laboratory of Regional Energy and Environmental Systems Optimization, Ministry of Education, North China Electric Power University, Beijing, 102206, China

[2]Institute for Energy, Environment and Sustainable Communities, University of Regina, Regina, Saskatchewan, S4S 0A2, Canada

[3]SC Institute for Energy, Environment and Sustainability Research, North China Electric Power University, Beijing, 102206, China

[4]School of Climate Change and Adaptation, University of Prince Edward Island, Charlottetown, Prince Edward Island, C1A 4P3, Canada

[5]School of Environment, Beijing Normal University, Beijing, 100875, China

Correspondence
Guohe Huang, Institute for Energy, Environment and Sustainable Communities, University of Regina, Regina, Saskatchewan S4S 0A2, Canada.
Email: huang@iseis.org
Xiuquan Wang, School of Climate Change and Adaptation, University of Prince Edward Island, Charlottetown, Prince Edward Island C1A 4P3, Canada.
Email: xiuquan.wang@gmail.com

Funding information
China National Key Research and Development Plan Project, Grant/Award Numbers: 2018YFE0196000, 2016YFA0601502, 2016YFC0502800; Environmental Protection Public Welfare Scientific Research Project, Grant/Award Number: 201509010; Fundamental Research Funds for the Central Universities, Grant/Award Number: 2017MS049

Abstract

Following its commitment to Paris Agreement in 2015, China has started to explore potential renewable energy solutions with low carbon emissions to mitigate global warming. Though wind energy is one of the most cost-effective solutions and has been favored for climate policy development around the world, its high sensitivity to climate change raises some critical issues for the long-term effectiveness in providing sustainable energy supply. Particularly, how wind speed and its energy potential in China will change in the context of global warming is still not well understood. In this paper, we simulate the near-surface wind speed over China using the PRECIS regional climate modeling system under different RCP emission scenarios for assessing the possible changes in wind speed and wind energy availability over China throughout the 21st century. Overall, the PRECIS model can reasonably reproduce the mesoscale climatological near-surface wind speed and directions as documented in reanalysis data across most regions of China, while some local discrepancies are reported in the southwestern regions. In the future, the annual mean wind speed would be decreasing in most regions of China, except for a slightly increase in the southeast. The expected changes in wind speed are characterized with different amplitudes and rates under different RCP emission scenarios. The changes in the spatial distribution of wind speed seem to be sensitive for RCP climate emission scenarios, especially in the late 21st century. The spatiotemporal changes in wind energy potential exhibit a similar behavior to those in near-surface wind speed, but the magnitudes of these changes are larger. In general, the wind power density is expected to increase by over 5% in winter in the major wind fields in China (ie, Northwest, North-central and Northeast), while significant decreases (by about 6% on average) are projected for other seasons (ie, spring, summer and autumn). By contrast, the wind energy potential in the northeast would increase over most months in the year, especially in winter and summer. The results of this research are of great importance for understanding where and to what extent the wind energy can be utilized to contribute renewable energy system development in China in support of its long-term climate change mitigation commitment.

KEYWORDS

China, high resolution, regional climate model, wind, wind energy potential

The peer review history for this article is available at https://publons.com/publon/10.1002/we.2417

1 | INTRODUCTION

Global warming in the past century is an indisputable fact, and the temperature is expected to continue to rise due to human activities.[1] Developing renewable energy is one of best ways to reduce emissions of greenhouse gases and is also an effective measure to mitigate and adapt to climate change. Renewable energy sources are sensitive to climate change itself. They are strongly influenced by weather and climate conditions, which might change significantly in the future.[2] Among these sources, wind is the second leading renewable energy source worldwide. In terms of installed generating capacity, fastest growth and technological maturity, only installed capacity by hydropower exceeds that of wind power generation.[3] With the increasing demand for renewable energy sources in the future, we must have a clear understanding of accessible wind resources and the susceptibility of these resources to climate change.[4]

China is rich in onshore and offshore wind resources, mainly distributed in the northeast, north, northwest and east coastal areas. According to the latest national wind resource evaluation results, China's technical exploitation amounts of wind resources with an 80 m height onshore wind power density of over 150 and over 200 W/m^2 are 10.2 and 7.5 TW, respectively. Taking factors such as resource potential in low wind speed regions and land resource constraints into account, China's total wind energy potential is estimated to 4899 GW onshore and 217 GW offshore.[5] In recent years, following its commitment to Paris Agreement in 2015, China has started to explore potential renewable energy solutions with low carbon emissions to mitigate global warming and has become the world's leader in wind power development. According to the latest annual market report by Global Wind Energy Council, China topped the 2017 global wind energy market in both new installed capacity and cumulative capacity, with 37% and 35% market share of the worldwide total, respectively (see online at http://gwec.net/cost-competitiveness-puts-wind-in-front/). However, wind energy resources are badly uneven in China and strongly dependent upon the strength of winds, which are determined by synoptic-scale variability and local processes to a large degree,[4] such as climatic and topographic factors. Therefore, it is desired to carry on the detailed investigation and evaluation of the available wind speed information in China.

Nowadays, increasing attention has been paid on the assessment of the wind energy potential around the world, such as North America,[6] Europe,[4,7] Africa[8] and East Asia.[9] However, simulation and projection of wind speed are very difficult because of its random and intermittent nature. Numerous studies have concentrated on developing effective wind speed simulating and forecasting models. Overall, these models are usually divided into two categories, namely, statistical models and physical models.

Statistical models usually employ the history samples to build some linear or nonlinear statistical relationships for fitting actual wind speed and are used to project the wind speed in short term. They are also classified into three types, including general regression methods, intelligent methods and hybrid forecasting methods. For example, Mao and Monahan[10] built the relationships between predictability of surface wind vectors and potential influential factors, such as topographic complexity, mean surface wind vectors and standard deviation and kurtosis of wind components, to analyze surface winds by linear statistical prediction. Shamshirband et al[11] developed a new auto-regressive model to capture chaotic dynamics of wind speed time series for a short-term (1-24 h) forecast. On the other hand, with the capability of self-learning and self-adaption, the artificial intelligence methods can capture some nonlinear characteristics of variables and have been used broadly. For example, Chang et al[12] presented an improved radial basis function neural network-based model with an error feedback scheme for forecasting short-term wind speed and power of a wind farm. Ileană et al[13] used an algorithm of data mining based on clustering to find different data categories in a wind farm data and further determined the most suitable prediction technique. However, most of the intelligent models are “black boxes” (no inside look at how things work), which could be their disadvantages in a sense. Thus, in recent years, hybrid forecasting methods are developed gradually. Niu et al[14] proposed a novel hybrid approach for multi-step-ahead wind speed forecasting utilizing optimal feature selection and an artificial neural network optimized by a modified bat algorithm with cognition strategy. Wang et al[8] combined the support vector regression, seasonal index adjustment and Elman recurrent neural network to form hybrid models for wind speed projection.

Nevertheless, there are some drawbacks in statistical models for wind speed simulation and projection: (a) most wind data is based on historical series (ie, meteorological observations, wind profiling lidar on platforms, remote sensing observations and reanalysis), which could be insufficient, especially in remote areas or complex terrains; (b) lacking a clear physical meaning, the statistical relationships are generally empirical; (c) near-term projection is more appropriate due to the assumption that the relationship built through historical data is applicable for future projection as well. Therefore, statistical models are most likely better at present climate wind assessment or short-term projection, while, in the context of a changing climate, physical models, especially climate models, can better answer how the wind resources will change in the future.

With respect to physical models in wind speed simulation, Carvalho et al[3] used a multi-model ensemble from IPCC CMIP5 to analyze the climate change impact on future European large-scale wind energy resource and found that the future large-scale wind resource would increase in Northern-Central Europe and decrease in the Mediterranean region. Similarly, based on global climate model simulations in the CMIP5 archive, Kulkarni and Huang[15] concluded that the current estimation of wind power potential for North America would not be significantly changed by the greenhouse gas forcing in the coming decades. Notwithstanding, there are a lot of uncertainties among these GCMs in simulation on the wind climatology attributed to their different physical mechanism and coarse spatial resolutions (over 100 km), especially for resolutions, which are vital for wind simulation influenced strongly by synoptic-scale variability and local topography easily. The detailed surface roughness at regional scale could not be included in the surface boundary conditions of GCMs.[16] Therefore, downscaling technologies are needed to get higher resolution wind data. Statistical downscaling is one of the most common methods, by establishing the mathematical relations between large-scale climatic

factors from GCMs to the local variables of interest. These methods are abundant and easy to use, and the downscaled resolution can reach a site scale.[17] However, as previously mentioned, statistical methods, which have no clear physical meaning and stationary relationships between predictors and predictands, may not be valid in an evolving climate.[18,19] Alternatively, the fine-resolution regional climate models (RCMs) with similar physical processes and mechanisms, which are nested into GCMs through dynamical downscaling technologies, can solve above problems well and produce more detailed local or regional climate information.[20] A number of papers have used RCMs to explore the changes in wind. Pašičko et al[2] used the climate data from the global climate model ECHAM5-MPIOM and dynamically downscaled by the regional climate model RegCM to assess the climate change impacts on energy generation from renewable sources in Croatia. Omrani et al[21] investigated the offshore wind energy potential over the North Western Mediterranean Sea in WRF regional climate system model, and the results showed that the simulated wind potential energy was very sensitive to the model configuration. Pryor et al[22] employed the RCAO model with boundary conditions derived from ECHAM4/OPYC3 and the HadAM3H to analyze the potential climate change impact on wind energy resources in northern Europe. Credible estimates of climate variables are the basis and premise of the assessment of the climate change impacts, while the high resolution of simulation is one of the decisive factors, especially for wind, precipitation and extreme climate variables, which are mainly subjected to regional terrains, vegetation, convection and so on. In terms of the importance of high resolution, Cantet et al[23] found that high-resolution simulation in temperature showed remarkable advantages over small islands. Lee and Hong[24] thought that the finer resolution model was more efficient in producing the major characteristics the precipitation distribution and temperature distribution. Dosio et al[25] found that the higher resolution simulation generally represented more intensity events, toward the right tail of the distribution. The PRECIS RCM system from Met Office Hadley Centre is one of most popular high-resolution RCMs. Nowadays, it has been widely utilized in a wide range of climate-related studies and impacts research projects across the world, and most of them focus on temperature, precipitation and their extreme[26-28] simulation and projection.

Studies on wind speed and its potential over China have emerged in the last few years. Based on observed wind records from wind measurement towers at six onshore sites with different geographical climate conditions in China, Li et al[29] used the Weibull distribution function to assess wind characteristics and wind energy potential. Wu et al[30] employed three probability density functions to model the wind speed distribution at a typical site in Inner Mongolia, China. Keyhani et al[31] assessed the performance of Intergovernmental Panel on Climate Change AR5 nine climate models in simulating and projecting wind speeds over China and considered that the wind speed in future spatial distributions were not significant differences relative those in history. Jiang et al[32] examined the capability of three RCMs to simulate the 10-m winds all over China in the late 20th century, concluded that they had the certain capability of imitating the distribution of mean wind speed but failed to simulate the greatly weakening wind trends in history.

Overall, a large number of climate model simulations of future wind change have been performed using GCMs or RCMs, and it is necessary to take into account the climate models at regional scale to simulate the geographic distribution or the inter- and intra-annual variability of the wind resource. Studies on high-resolution regional climate modeling for wind energy assessment are very limited. This is especially true for China. To our best knowledge, studies on RCM simulations at high resolution and long-term continuous for the whole country of China are very few, even though the resolution of well-known CORDEX for East Asia is only approximately 50 km.

Therefore, to complement the existing studies, here we use the PRECIS regional climate modeling system at its highest spatial resolution (25 km) to investigate the possible changes in wind pattern over China in response to global warming. The performance of the model is first evaluated through detailed comparison with the ERA-Interim reanalysis data. The future changes in the spatial and temporal patterns of wind speed and wind energy potential across the country are analyzed afterwards. The results can provide useful information to relevant government departments for making better decisions for onshore wind energy developments and mitigation strategy response to climate change in future.

2 | DATA AND METHODS

2.1 | PRECIS regional climate model

Developed by the Met Office Hadley Centre, as a RCM, the Providing Regional Climates for Impacts Studies (PRECIS) has been widely utilized to produce detailed climate projections, owing to its easy-to-use and wide suitability in any chosen region of the world.[20,33] PRECIS has 50- and 25-km resolutions at the equator of the rotated regular latitude-longitude grid and contains 19 levels in the vertical. The outputs from the second version of the Hadley Centre Global Environmental Model (HadGEM2-ES), which is coupled ocean-atmosphere GCM and Earth System Model with 38 vertical levels and horizontal resolution 1.875° × 1.25°,[34] under RCP4.5 and RCP8.5 scenarios are introduced as the lateral boundary conditions to drive the PRECIS. The land surface scheme employs Met Office Surface Exchange Scheme 2.2 (MOSES 2.2).[34] PRECIS is a high packaged and integrated model system, and has its own physical parameterization schemes, including dynamical flow, the atmospheric sulphur cycle, clouds and precipitation, radiative processes, the land surface and so on. A mass flux penetrative convective scheme[35] is used, including the direct impact of vertical convection on momentum (in addition to heat and moisture)[36]. The radiation scheme includes the seasonal and diurnal cycles of insolation, computing short wave and long wave fluxes.[37,38] In this paper, we use the latest version of PRECIS (PRECIS 2.0) and run continuously from 1950 to 2099 at its high spatial resolution (25 km).

2.2 | Wind data and validation method

To provide independent assessment of the PRECIS output during the historical period, we use the daily 10-m wind speed from the u and v wind components from the European Centre for Medium-Range Weather Forecasts Interim Reanalysis (ERA-Interim) data set. It is a popular global atmospheric reanalysis from 1979, continuously updated in real time. The spatial resolution of the data set is approximately 80 km on 60 vertical levels from the surface up to 0.1 hPa.[39] The data can be found at https://www.ecmwf.int/en/forecasts/datasets/archive-datasets/reanalysis-datasets/era-interim. At present, the ERA-Interim reanalysis materials have been used widely for wind energy assessment in China.[40-42] In this paper, the reanalysis data is remapped to the same resolution grids as those of the PRECIS output for comparison.

For evaluation metrics, we use mean absolute error (MAE), mean relative error (MRE) and the Taylor Diagram[43] to quantify the performance of the PRECIS model in the baseline period. For the future projection, a non-parametric Mann-Kendall statistical test[44] is used to analysis the tendency of wind speed in future, and the Theil-Sen trend estimation method[45] is used to calculate the magnitude of trends.

In the real world, typical wind turbines are placed at 80 m (or higher) above ground or mean sea level, while most climate models can only provide near-surface (10 m) wind output, not excepting PRECIS. Since 10 and 80 m winds are highly correlated, the former is often considered as the best proxy of the wind at typical wind turbines height.[3,46] However, when we analyze the wind energy potential changes in the future over China, we transform the 10 m wind speed to 80 m hub height by the mathematical formula,[6,22] as follows:

$$v = v_r \left(\frac{z}{z_r}\right)^{\alpha} \tag{1}$$

where v is the wind data at hub height, v_r is the wind data simulated by PRECIS, $z$and $z_r$are hub height and simulated wind speed height and α is the wind shear exponent of 1/7.

The wind power density is usually used as an indicator for wind energy potential, which is derived from the 80 m wind speed following equation[31]:

$$E = \frac{1}{2}\rho U^3 \tag{2}$$

where$E$ is the wind power density (W m^{-2}), ρ is the air density (kg m^{-3}) and U is the wind speed at height of 80 m (m s^{-1}).

The study domain contains about 40 000 25-km grid points and is divided into six sub regions based on their typical geographical climate conditions, which are the northwest (NE), north central (NC), northeast (NE), west (W), central (C) and southeast (SE) of China (Figure 1). The northern three regions (NW, NC and NE) are regarded as the major onshore wind power farms in China. We selected the continuous dataset of the period

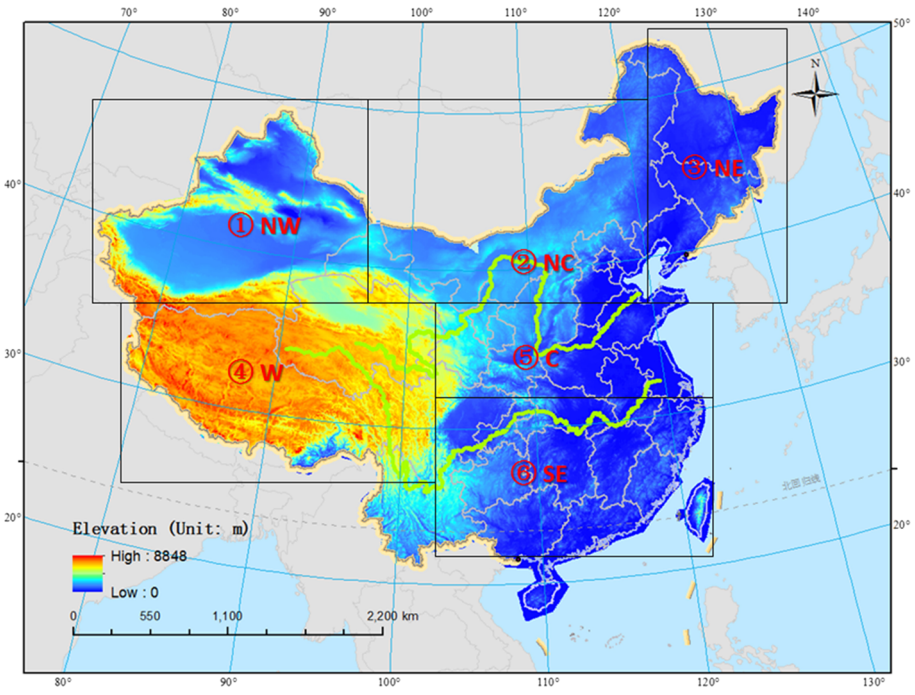

FIGURE 1 Study domain for the regional climate model output. Six sub regions are selected for analyzing across different climatic regions of China, which are northeast (NE), north-central (NC), northwest (NW), west (W), central (C) and southeast (SE), respectively

1979-2005 as the baseline period for model validation, and the years of 2011-2040 (2020s), 2041-2070 (2050s) and 2071-2099 (2080s) as the near-, mid- and long-term periods of 21st century for future projection under RCP4.5 and RCP8.5 emission scenarios. In addition, some abbreviations are defined as follows: annual (ANN), spring (March, April and May, or MAM), summer (June, July and August, or JJA), autumn (September, October and November, or SON) and winter (December, January and February, or DJF).

3 | RESULTS

3.1 | Model validation

Figures 2 and 3 show the spatial distribution of annual and seasonal mean near-surface wind speed in observation, simulation and their biases (including absolute and relative errors) during the baseline period. Overall, the PRECIS model can reasonably reproduce the mesoscale climatological 10-m wind speed patterns across most regions of China aside from local discrepancies, especially in southwestern regions. The main wind field centers of China (the north and west) are well simulated by PRECIS, with −0.3 ~ 0.6 m/s absolute errors and −10% ~ 30% relative errors approximately (Table 1). The annual mean wind speed simulated by PRECIS exhibits differences in spatial distribution. For example, the annual mean wind speed is underestimated in the north and the east of Tibet Plateau, while some obvious positive biases are found in the western margin of Xinjiang, the southeast of the Tibet and the west of Sichuan. The relative error in the west is the largest (above 30%). The wind speed in most parts of the SE of China is also slightly overestimated relative to the observation. Among these six sub regions, despite underestimated, the errors (about 10%) in the NE, NC and NW are smaller than other regions, meaning that the PRECIS has a good performance in simulating near-surface wind speed in the major wind power farms of China. Figure 2 also depicts the annual mean wind directions over China and shows that the PRECIS correctly captures the predominance of southwesterly flow observed in reanalysis data, particularly in the west and northeast of the domain. However, the trend seems to be large and noisy relative to the observation in virtue of higher resolution and detailed topographic effects in simulation.

The comparison in seasonal mean wind speed is similar to that in annual between simulation and observation. The biases are negative in the north and positive in the south of China. Besides from summer, the results simulated by PRECIS are seriously overestimated in the western margin of Xinjiang and the west of Sichuan but slightly underestimated in most regions of the north. For the reasons, the PRECIS also shows a worse skill

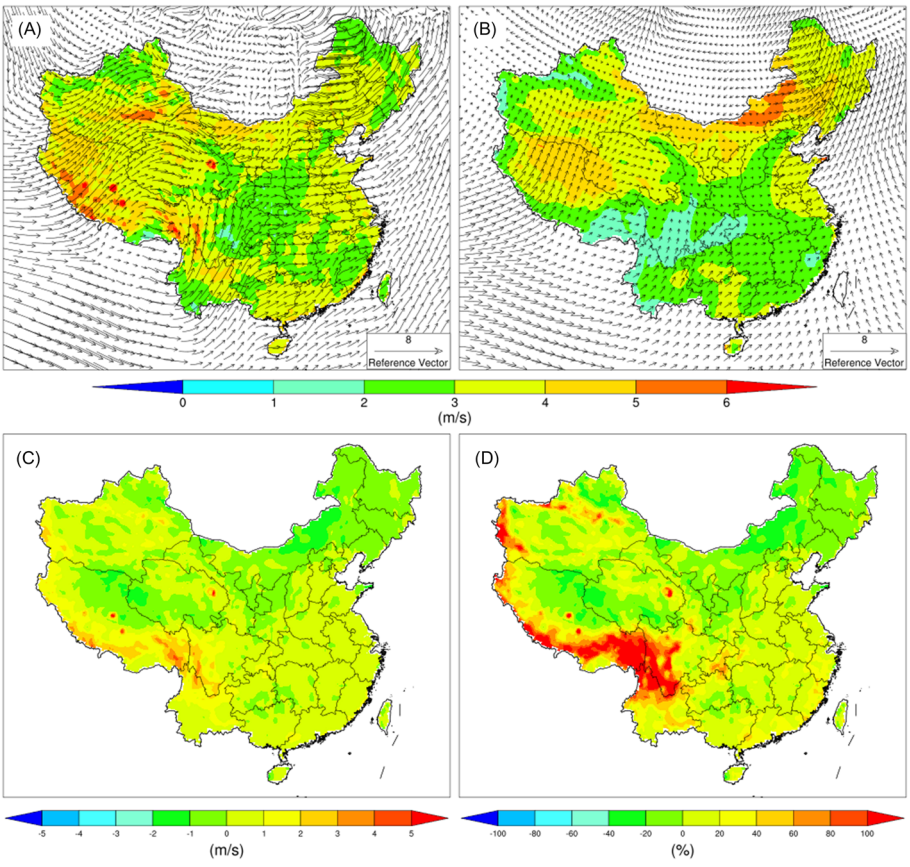

FIGURE 2 Spatial distribution of annual mean wind speed and direction during the baseline period: A, PRECIS; B, ERA; C, absolute bias; D, relative bias

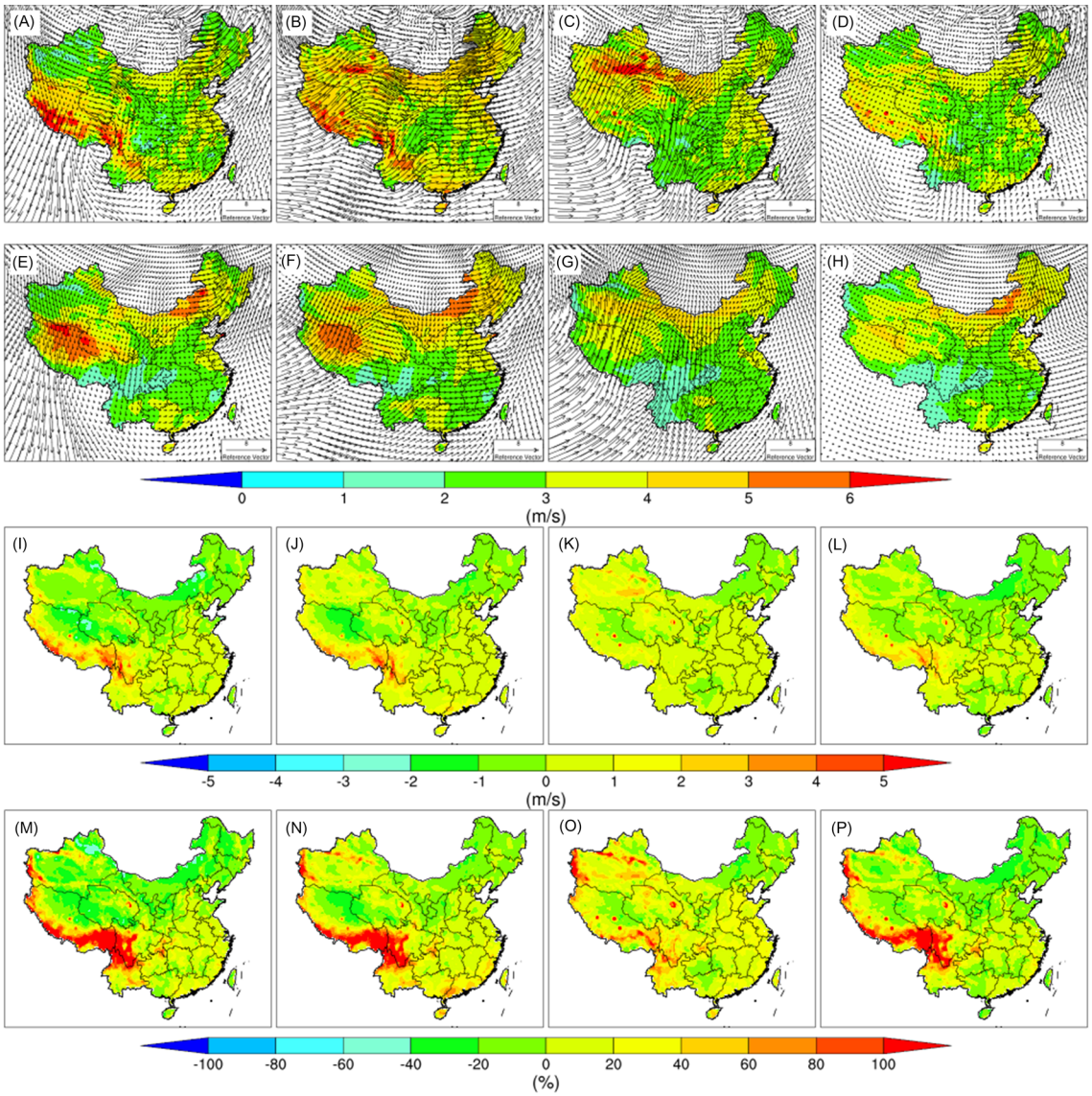

FIGURE 3 Spatial distribution of seasonal mean wind speed and direction during the baseline period: A-D, PRECIS; E-H, ERA; I-L, absolute bias; M-P, relative bias. From left to right, each column represents winter, spring, summer and autumn

TABLE 1 Regional mean absolute (m/s) and relative errors (%) in near-surface wind speed for different regions and seasons

Region	ANN	DJF	MAM	JJA	SON
China	0.195/11.398	0.011/6.892	0.301/14.387	0.387/15.722	0.080/8.385
NW	0.252/11.180	−0.300/−6.505	0.382/14.167	0.858/28.205	0.068/5.656
NC	−0.287/−5.643	−0.550/−12.104	−0.185/−3.033	0.063/3.248	−0.477/−10.663
NE	−0.301/−8.999	−0.435/−13.468	−0.184/−5.042	−0.123/−4.211	−0.461/−13.283
W	0.648/33.792	0.665/39.718	0.665/34.876	0.478/22.925	0.785/39.909
C	0.229/8.995	0.163/6.775	0.197/7.304	0.464/17.998	0.092/4.405
SE	0.413/15.370	0.407/15.925	0.644/23.970	0.362/15.302	0.239/10.178

Note. The left values are absolute error (m/s) and the right values are relative error (%).
Abbreviations: ANN, annual; DJF, December, January and February; JJA, June, July and August; MAM, March, April and May; SON, September, October and November.

in the whole west than that in the east. As a whole of China, the relative errors are smaller in fall and winter (about 6%~8%) than those in spring and summer (about 14%~15%) (Table 1). In spring, the wind speed simulated by PRECIS in the NC and NE is close to observation (smaller about 3%~5%), especially in the NC with MAE of −0.185 m/s and MRE of −3.033%. As can be seen, wind directions are obviously disparate at the different seasons. Compared with the observation, the predominant wind directions in four seasons are simulated well by PRECIS over most regions of China. The most frequently wind directions are from north to south in winter and the east and northeast wind are mainly in spring. The summer wind direction is dominated by southerly wind component. The trend of wind directions in autumn is evenly distributed and smaller than that in other seasons.

In order to further quantify the PRECIS's ability on simulating the pattern of the wind speed over China during the baseline period, a Taylor diagram is used to represent correlation coefficient, the centered pattern root-mean-square difference and the ratio of standard deviations between the simulation and observation for present-day annual and seasonal mean wind speed (Figure 4). The pattern correlation coefficients over most regions are 0.5 ~ 0.9 except the west. The simulated results in the east of China (ie, NE, NC and SE) are more closely correlated with observation than in the west, particularly for the NC with the correlation coefficient of 0.9 approximately. The ratio of standard deviations is close to 1.0, especially in summer (except for NC and NW), indicating the pattern variations simulated by PRECIS are similar with observation. The RMSE is in the range of 0.5 ~ 1.0 m/s for most regions and seasons. Overall, the errors in the NC, NE and C are smaller than other regions.

Figure 5 shows the monthly mean wind speed as simulated by PRECIS over China and its six sub regions relative to observation. Although RCM is overestimated to some degree in most months, the monthly mean peak and valley wind speed, that is, the highest wind speed appears during the spring months (ie, March or April) and the lowest appears in summer (ie, August), which is consistent between RCM and observation. On the whole China, during some relative cold months (ie, January, October, November and December), the results from PRECIS show a better performance than other months, with near zero MAE and MRE of about 5% (Figure 5A). On the other hand, there are some differences in predefined six sub regions. Specifically, there is a negative bias (about 15%) in the northeast, especially in July. Also, similar bias is in the NC (Figure 5C), though a slightly positive bias between PRECIS and observation is found in July and August. Relatively larger bias is in the western China and the MRE is even more than 20% in September and October (Figure 5E). In the northwest, there is an inconsistency between PRECIS and observation in summer, when the mean relative error is even exceeding 30% (Figure 5B). It is suggested that the PRECIS still has some deficiencies in simulating for the NW in this season, which is also be identified from aforementioned Taylor diagram. In general, compared with some regions of China (ie, NC and NE) with weak negative biases, the mean wind speed in others areas of China is completely overestimated with excessively positive biases in all months throughout the year, especially in west. Thus, it also can explain why the mean wind speed is overestimated in the whole of China.

3.2 | Projections of wind speed and wind energy potential

3.2.1 | Changes in near-surface wind speed

Figure 6 represents the annual changes of near-surface wind speed in spatial distribution over China during the 21st century under different RCP emission scenarios. In the early 21st century, there is a not very clear change in spatial distribution for annual mean wind speed, ranging from −2% to 2%. In the mid-late stage of 21st century, except for a slightly increase in the SE, most of China's wind speed would be decreased, especially in the Tianshan Mountains nearby and the southwest of the Tibet Plateau. It should be noted that the wind speed changes appear to be sensitive for RCP climate emission scenarios, especially in the late 21st century. In other words, in the same period, both increasing and decreasing tendencies intensify as the greenhouse gas forcing is enhanced.

As shown in Figure S1 (see Supplementary Information), the mean wind speed of winter would be increased over most regions of China, such as in the NW, NE and southern of Guizhou. The increase of speed wind could be even as high as 8% in the parts of Xinjiang in the late 21st century. On the other hand, similar with changes in annual mean wind speed, the decreasing trend would occur in the southwestern of Tibet and most area of Yunnan, reducing by about 2%, 6% and 8% in the next three periods under RCP4.5, respectively. The changes under RCP8.5 are larger than those under RCP4.5. The changes of wind speed in spring are also varied in space-time distribution (Figure S2). In the early 21st century, a slight increase is found in the west of China but decreasing in the following two periods. There is a declining trend in the NC and NE region obviously, particularly in the east of Inner Mongolia and northeast corner of China (decreasing by over 4%). Under RCP4.5, the wind speed in the central regions of China would increase by 2~4% and exhibits a trend of southeastward expansion from the middle of this century. In the late 21st century under RCP8.5, the decrease in the southeast of Tibet is quite apparent. The distributions in autumn are similar with those in spring, though larger decrease in the Tibet Plateau and the south of Yunnan (Figure S4). The differences in summer from other seasons in spatial distribution are over the southern regions of China (ie, the C, SE and Yunnan), where the wind speed would increase obviously, even more than 10% in some regions. In addition, the increase (about 2%) is also found in the NE region by the end of this century. Such a projected increase of the mean wind speed in future climate could potentially have large impact on electricity production in these regions. In summer, the changes in the NW and Inner Mongolia are consistent with those in other seasons (Figure S3).

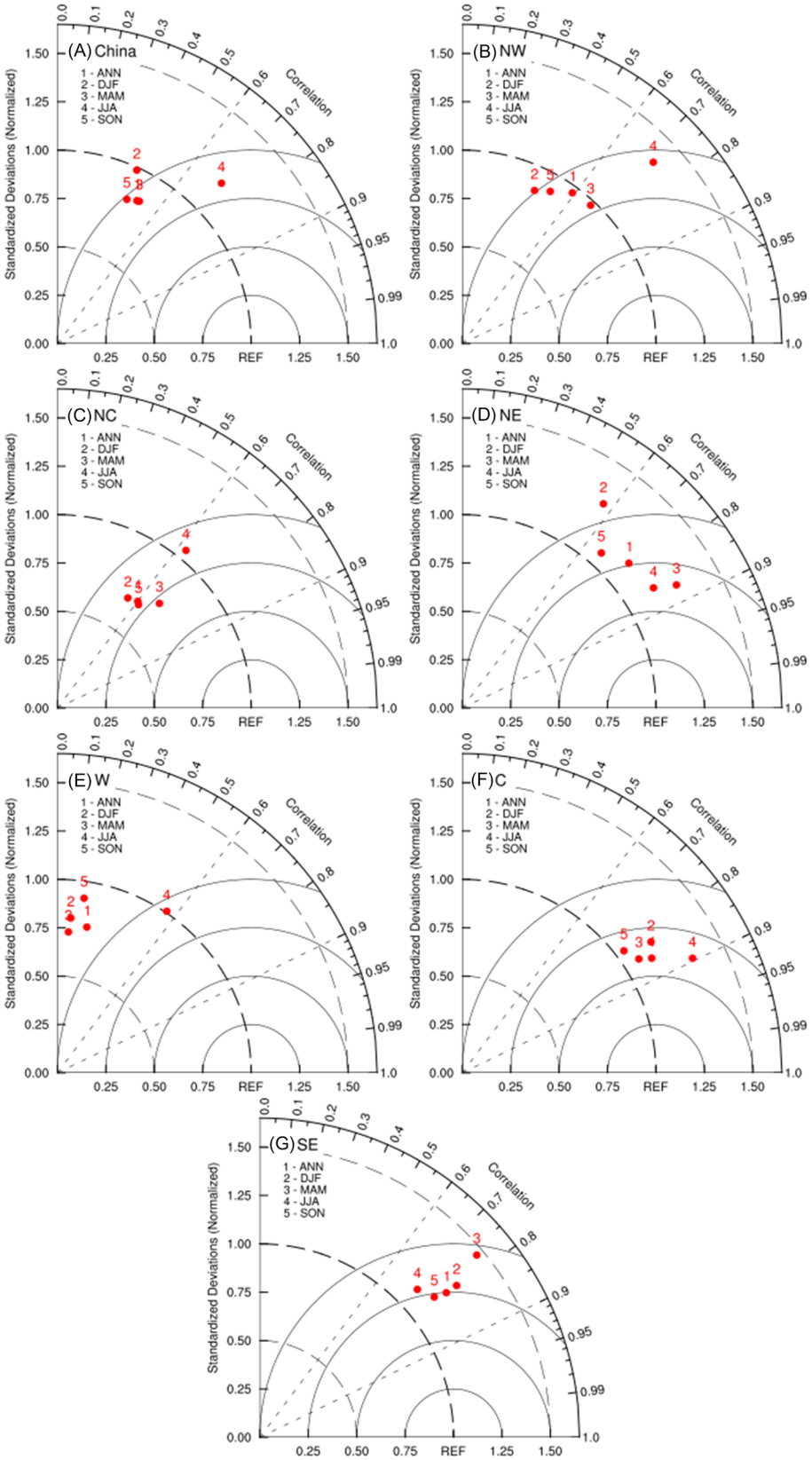

FIGURE 4 Taylor diagrams of mean annual and seasonal wind speed for simulation versus observation over the entire China (A) and six sub regions (B-G)

The wind speed changes in annual cycle in the next three periods for different regions are shown in Figure 7. At the national scale, except for slight increase for several months in winter (ie, January and December), the near-surface wind speed is likely to be decreased relative to the baseline, especially in May (reducing by over 3%), September and October (reducing by 2%~3%). The monthly changes in wind speed differ among six sub regions. In the NW region, except an increase in winter (January, February and December), the wind speed would decrease in other months

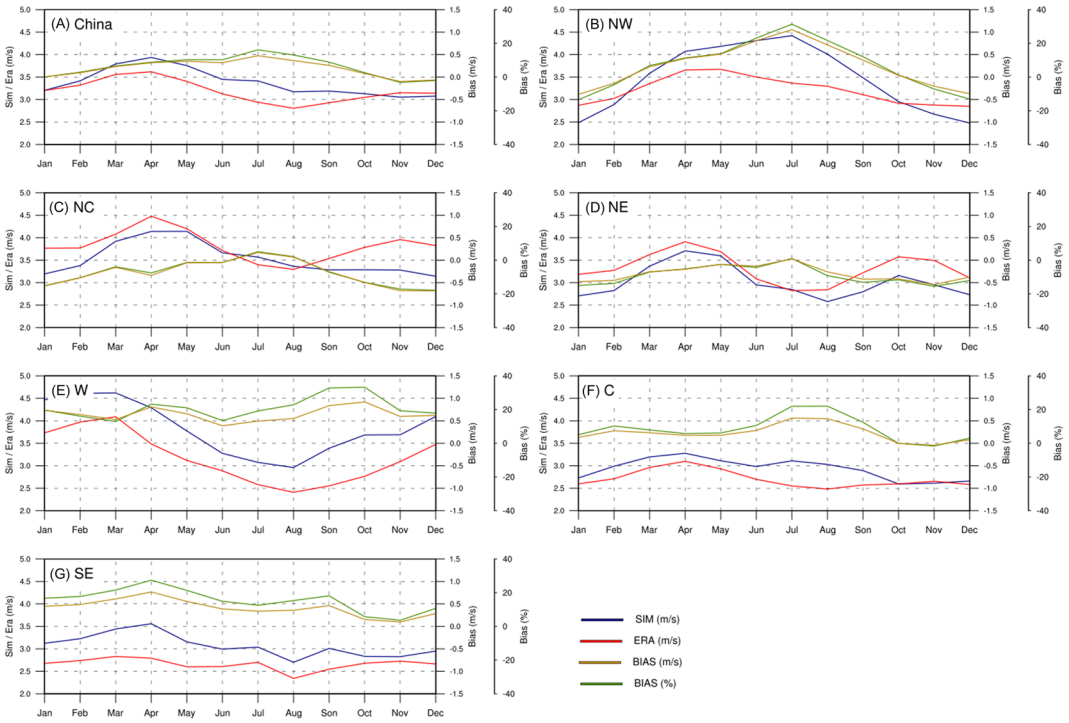

FIGURE 5 Annual cycle of absolute biases (yellow) and relative biases (green) in mean wind speed between simulation (blue) and observation (red) over China and six sub regions during the baseline period. A, whole China; B-G, sub-regions

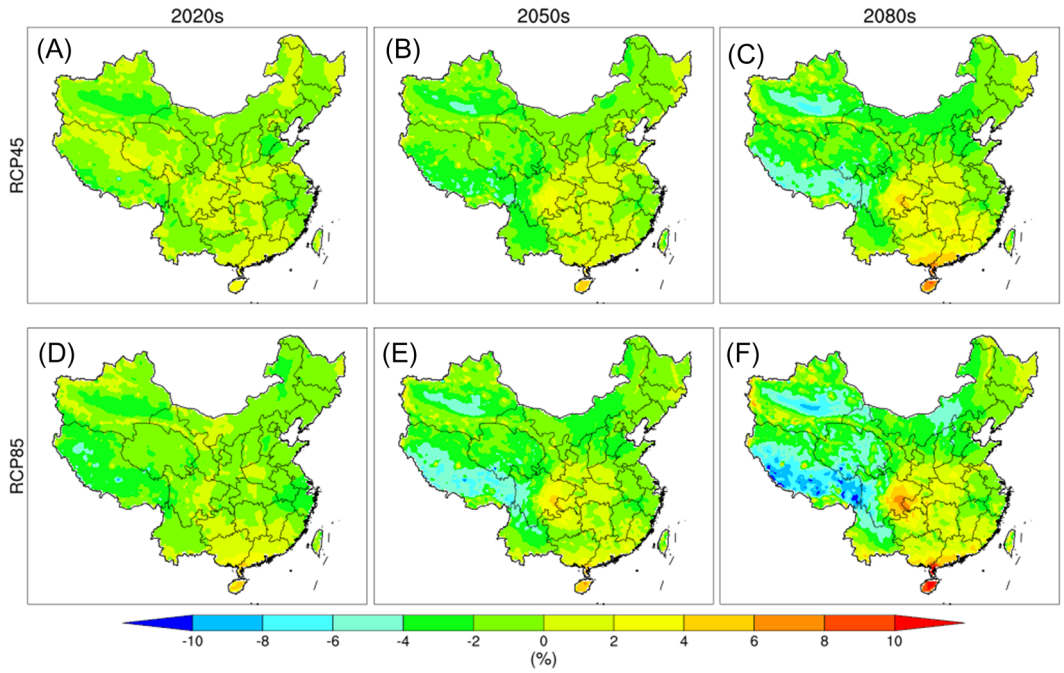

FIGURE 6 Projected changes (unit: %) in spatial distribution for annual mean near-surface wind speed. Columns from left to right are shown as 2020s (A, D), 2050s (B, E) and 2080s (C, F) and rows from first to second are shown as RCP4.5 (A-C) and RCP8.5 (D-F) emission scenarios, respectively

with the lowest at June and July (about −4%). In January and February, the wind speed would increase slightly in the NC region where China's main wind power fields are located, but most of the time, the wind speed in future are smaller than that in the baseline period. It is worth outlining that the spread range of monthly mean wind speed in the NE region is larger than that in other regions. Except for a few months (ie, May, September and October), in colder months (ie, January, February, November and December) and warmer months (ie, July and August), the wind

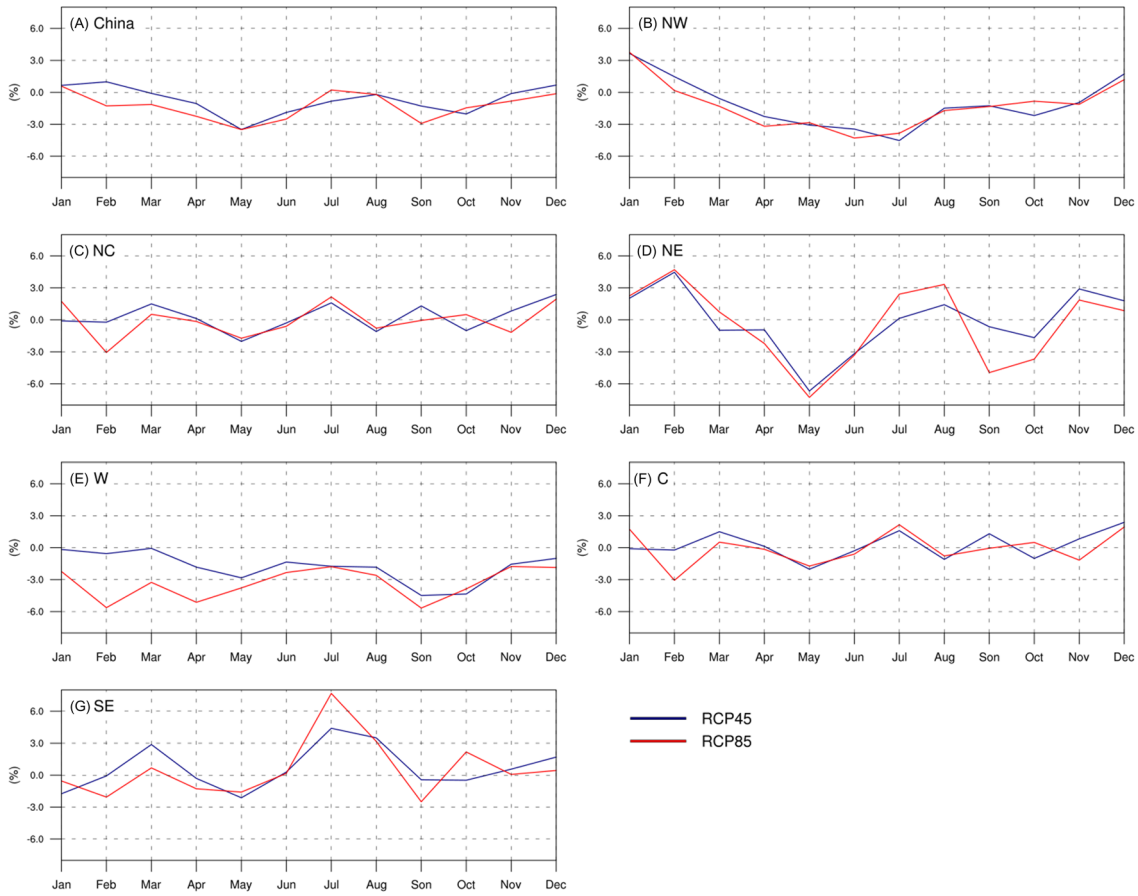

FIGURE 7 Annual cycle of regional mean near-surface wind speed over the whole China (A) and sub-regions (B-G) under RCP4.5 (blue) and RCP8.5 (red)

speed would be increased obviously (Figure 7D). Regardless of which emission scenarios, for the west region, the monthly wind speed through the year in future is likely to be smaller than that in the baseline period, and the changes in the first months seem to be more under RCP8.5 than RCP4.5. The wind speed in the NC region has a little change, ranging from ~ −2% to 2%. The result shows that the mean wind speed peak in annual cycle for the SE region is in July under RCP8.5, increasing by over 8%. Overall, apart from a few months (ie, February), the emission scenarios do not affect the changes of wind speed in annual cycle as much as in seasonal spatial distribution.

Figure 8 shows the inter-annual changes of near-surface wind speed averaged over the whole of China and six sub regions relative to the baseline period. Averaged over the whole China, the wind speed would show a slight descending trend in this century, and the magnitudes and inter-annual variability of wind speed are different according to the emission conditions. The domain averaged wind speeds for sub regions computed for two RCP scenarios also show different temporal trends. For example, the change rate is positive in the SE and C regions but negative in the NW, NC and W regions. The tendency is different for the NE region. Under RCP4.5, the wind speed is likely to decrease by 0.012% per year, while opposite trend is under RCP8.5. The largest decrease magnitude and rate in regional averaged wind speed are found in the west region of China, where the wind speed would reduce by about 6% by 2100 with a rate of 0.048% per year under the RCP8.5 scenario.

3.2.2 | Changes in wind energy potential

Generally, the changes in wind power density are larger than those in wind speed.[2,47] Here, we focus the changes in wind power density in the north three regions (ie, NE, NC and NW) based some reasons as follows: (a) The major wind power fields of China locate in the north regions, such as Xinjiang, Inner Mongolia and Northeast;[48] (b) though the mean wind speed is large in the Tibet Plateau, its actual wind energy potential is small owing to its high altitude resulting in low wind power density; and (c) the wind speed in the central and southeastern onshore regions is smaller than that in the north of China, though the wind energy resources is also rich in coastal area of southeast, the offshore wind speed is not in the scope of this study.

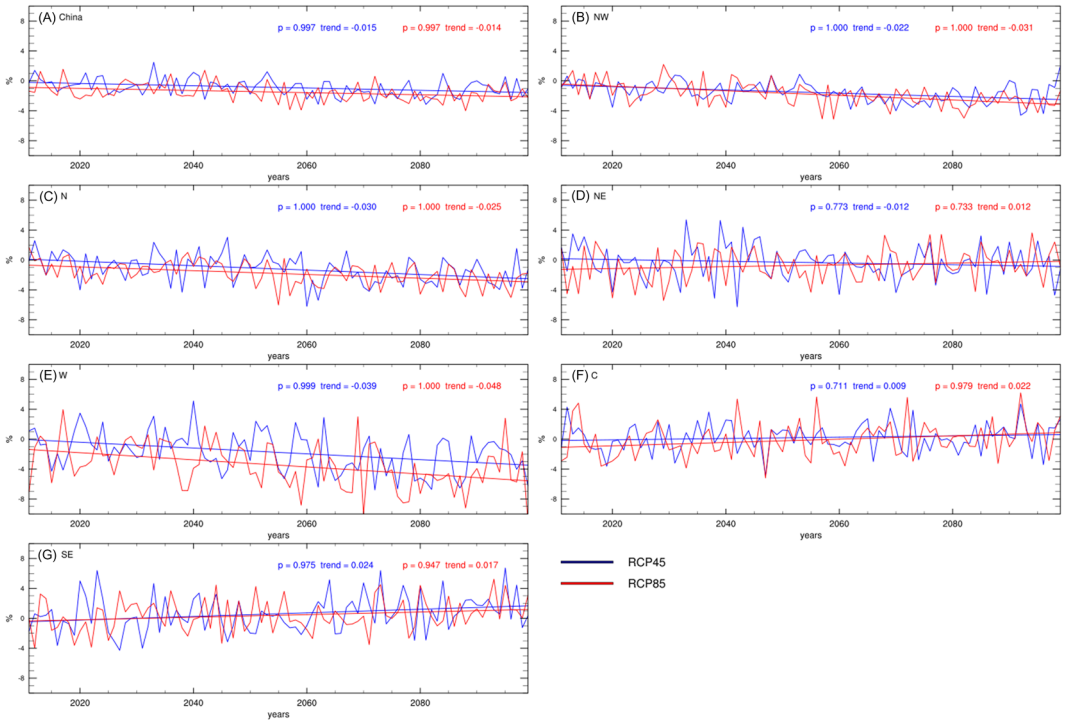

FIGURE 8 Annual changes of near-surface wind speed averaged over the whole of China (A) and six sub regions (B-G) relative to the baseline period. Colored straight lines show MK linear trends. The blue line represents trend under RCP4.5 and the red line represents trend under RCP8.5 (unit: %/year)

The space-time distribution changes in annual mean wind power density at 80 m height under different future periods and RCP emission scenarios are presented in Figure 9. The results show the wind energy potential would be reduced by over 10% in the southern Xinjiang and southwest of the Tibet Plateau. However, the southeast region is likely to have an increasing tendency. Although these space-time distribution changes in mean wind energy potential exhibit a similar behavior with those in near-surface wind speed, the change range is larger and the response to climate emission scenarios is also more sensitive. For example, it is noticed that the wind energy potential would decrease obviously in the west, northwest and central of Inner Mongolia of China under the RCP8.5 emission scenario from the mid and late twenty-first century, while there would be an obvious increase in the wind power density in the southeast regions, especially in the east of Sichuan.

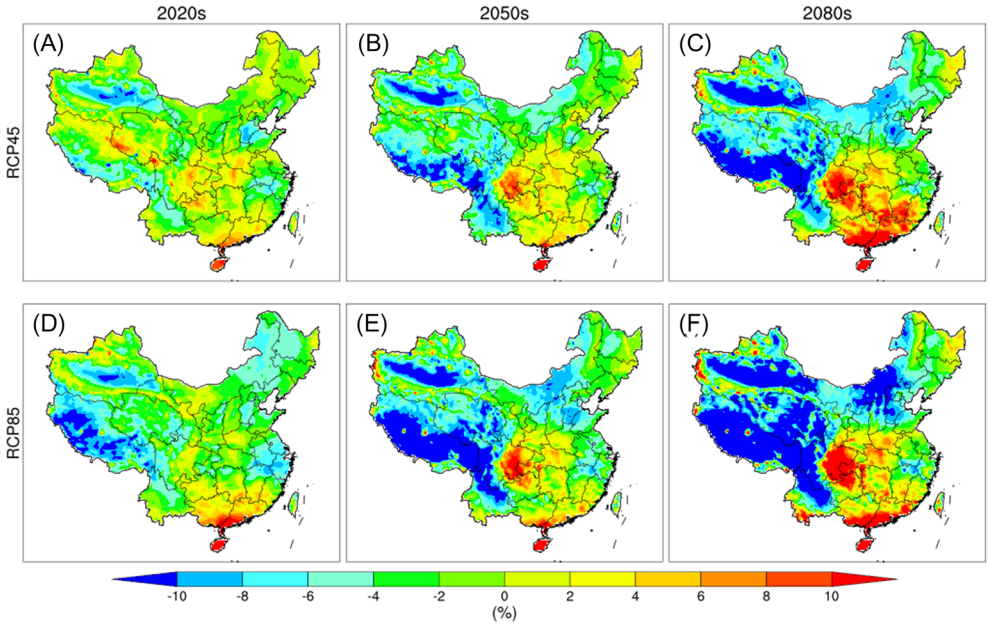

FIGURE 9 Projected changes (unit: %) in spatial distribution for annual mean wind power density at 80 m height. Columns from left to right are shown as 2020s (A, D), 2050s (B, E) and 2080s (C, F) and rows from first to second are shown as RCP4.5 (A-C) and RCP8.5 (D-F) emission scenarios, respectively

The seasonal changes of wind power density in future are shown in Figures 10 and S5-S7. The results indicate that the seasonal space-time distribution of wind energy potential is broadly in line with that of near-surface wind speed but has more change ranges. Significant differences between seasons are detected. In winter, the wind power potential would increase by over 5% in the three regions of northern China (Figure 10), while significant decreases (by about 6% on average) are projected for other seasons (ie, spring, summer and autumn). For example, the wind power density over the NE region in winter would be raised by 11.66% in the middle of this century under RCP4.5 and 14.53% in the end of this century under RCP8.5 (Table 2). On the other hand, in most southeastern regions, such as Tibet and Yunnan, an apparent decrease in the wind power density is found and even down more than 10% in some local areas. The similar distribution is observed in spring and autumn. Overall, the wind power density would decrease over China, except for small regions in the SE. In the end of this century, the density would be reduced by 8.75% in the NW, 9.62% in the NC and 9.85% in the NE under RCP4.5, and even more decreases under RCP8.5. In summer the increase or decrease of wind power density in spatial distribution seem to be just the opposite relative to that in winter. A general increase would be occurred in the SE region while a decrease in the most regions of northern China. Nevertheless, the NE region is an exception, where the wind energy potential would increase by 2.43% under RCP4.5 and 6.64% under RCP8.5 in the end of this century.

Figures S8 and S9 show the monthly changes and annual tendency in the wind power density over the entire China and northern three sub regions compared with the baseline period under different RCP emission scenarios, respectively. Despite larger magnitude, it can be observed that the variation pattern of the wind power density strictly follows that of the mean wind speed. In annual cycle, over the whole of China, the wind energy potential would be smaller in future than that in the baseline period in most months. The largest amplitude of change is found in May, with

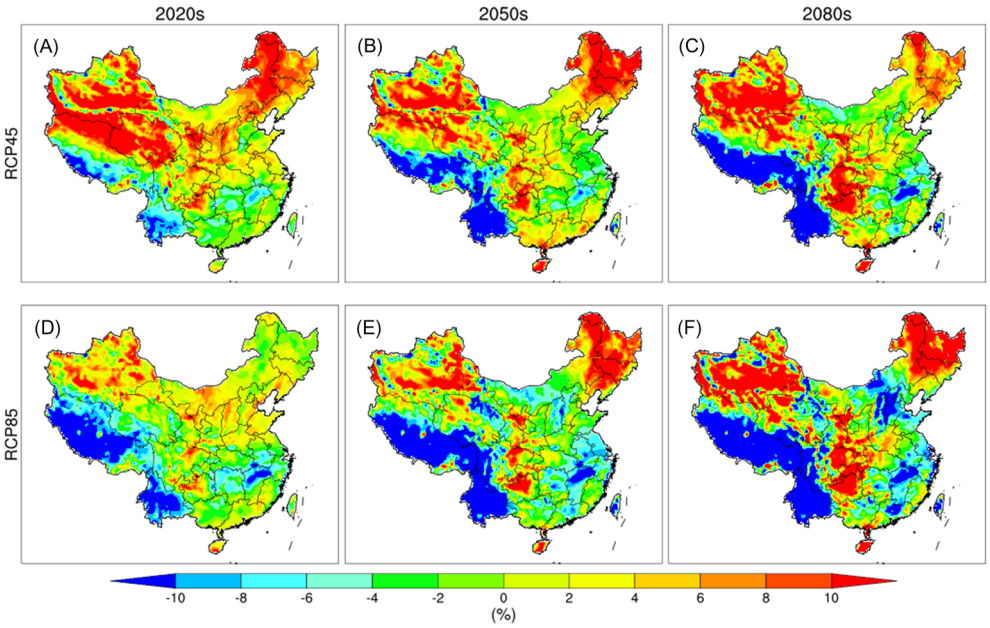

FIGURE 10 Projected changes (unit: %) in spatial distribution for mean wind power density in winter. Columns from left to right are shown as 2020s (A, D), 2050s (B, E) and 2080s (C, F) and rows from first to second are shown as RCP4.5 (A-C) and RCP8.5 (D-F) emission scenarios, respectively

TABLE 2 Regional mean changes (%) in wind power density for different regions and seasons

		RCP4.5				RCP8.5			
Region	Period	DJF	MAM	JJA	SON	DJF	MAM	JJA	SON
NW	2020s	7.11	−3.06	−7.44	−3.53	3.75	−4.00	−5.95	−1.62
	2050s	5.27	−6.28	−8.29	−3.70	3.60	−6.27	−9.00	−3.51
	2080s	8.57	−8.75	−11.55	−6.04	7.80	−11.45	−12.81	−5.10
NC	2020s	5.33	−4.21	−6.61	0.85	2.00	−4.12	−5.88	−2.57
	2050s	2.41	−6.22	−6.40	−0.65	−0.53	−5.01	−9.59	−5.51
	2080s	0.74	−9.62	−7.78	−5.62	−1.38	−9.93	−7.66	−9.57
NE	2020s	7.80	−7.50	−3.00	4.38	0.45	−8.16	1.03	−4.80
	2050s	11.66	−7.83	−4.80	−1.17	10.08	−8.49	−1.27	−4.69
	2080s	6.49	−9.85	2.43	−1.59	14.53	−9.45	6.64	−10.32

Abbreviations: DJF, December, January and February; JJA, June, July and August; MAM, March, April and May; NC, north-central; NE, northeast; NW, northwest; SON, September, October and November.

a 10% decrease approximately. Under RCP4.5, the wind power density could increase slightly in some months (ie, winter, below 5%). The falling speed of wind power density between two emission scenarios is different, with −0.042% per year under RCP4.5 and −0.038% per year under RCP8.5. In the NW region, except for winter months, future monthly wind power density would decrease obviously in most months of the year relative to the baseline period, especially from April to July. The general annual change trend is also downward in the NW region. The speed rate is almost extensively identical under two RCPs in the early 21st century, but the falling speed would be faster under RCP8.5 than RCP4.5 from 2050. Unlike in the NW region, the variation range of the wind power density in annual cycle is smaller in the NC, even though they both have a downward trend in annual mean. Compared with the baseline period, the increased months (exceeding six) in the NE region show more than other regions. In the annual mean, though the wind power density is smaller in the beginning of this century than that in the baseline period, we noted that the wind power density would increase gradually with the rate of 0.037% per year under RCP8.5. It is very meaningful to further explore the wind energy resources in the NE region for China, especially in the environment where the mean wind speed is generally reduced on the whole China in future.

4 | DISCUSSION AND CONCLUSIONS

In this paper, we simulated the near-surface wind speed over China using the PRECIS regional climate modeling system under different RCP emission scenarios. The main objective of this paper is to assess the possible future change of the wind speed and the resulting wind energy availability over China throughout the 21st century.

Overall, the PRECIS model can reasonably reproduce the mesoscale climatological near-surface wind speed and directions as documented in reanalysis data across most regions of China, while some local discrepancies are reported in the southwestern regions. In terms of spatial distribution, whether annual or seasonal mean, the PRECIS underestimates the wind speed in the north while overestimates in the south of China. Compared with the baseline period, the largest biases were found in the west regions, especially in the western margin of Xinjiang, the southeast of Tibet and the west of Sichuan. It is really difficult to simulate or project the climatic change (including temperature and precipitation) in these regions. On the one hand, due to the complex and inaccurate land surface information, many large and inevitable errors appear in the climate models, which is the main reason for above questions.[49] On the other hand, the meteorological stations as observations are still sparse over high topographic regions. In addition, we also noted that the near-surface wind field is overestimated obviously in these regions. This could because the resolution of PRECIS is higher than ERA-Interim reanalysis. Wind speeds can vary significantly in high-resolution models,[21,50] that is, the complex surrounding orography (ie, mountains and valleys) is smoothed by coarse-resolution reanalysis in the high elevation areas, resulting in less constrained and less channeled by the smoothed orography, which explains the stronger wind speed in the PRECIS simulation.

In future, the changes in annual and seasonal mean near-surface wind speed would vary in spatial distribution. Except for a slightly increase in the southeast, the annual mean wind speed would decrease in most regions of China, especially in the Tianshan Mountains nearby and the southwest of the Tibet Plateau, which is similar with that in spring and autumn as well. The regional spatial changes for annual wind speed are in line with those in global scale, such as, the decreases in wind resources across the Northern Hemisphere mid-latitudes and increases across the tropics and Southern Hemisphere.[51] These different patterns can be explained by polar amplifications and enhanced land-sea thermal gradients. However, in this paper, we also found that the mean wind speed would increase over most regions of China in winter, especially in the north areas.

In terms of the trend, the annual mean wind speed across China would decrease gradually throughout the 21st century and be characterized with different amplitudes and rates under different RCP emission scenarios. The reasons are manifold, one of which is the temperature. At present, many research literatures support that the regional changes in continental wind field are linked to large-scale dynamical and thermodynamic mechanisms governing the overall response of the atmospheric general circulation to radiative forcing changes in surface temperature.[51] Increasing of temperatures in land regions could decrease the atmospheric pressure at near-surface levels and weaken the temperature and pressure gradients between the land and adjacent oceans. Weakened pressure-gradient force drives weaker winds, resulting in the wind speed decrease.[52] It is well known that the mean temperature will continue to rise in the high probability over China in future under the context of global warming.[1] Therefore, a cause of the dominant trend of wind speed decrease across China may originate from the future temperature increases.

We also found that the changes in annual or seasonal spatial distribution of wind speed seem to be sensitive for RCP climate emission scenarios, especially in the late 21st century. However, the increasing radiative forcing does not give an apparent response to wind climates in annual cycle. It is controversial whether wind changes are response to climate emission scenarios. Chen et al[53] evaluated multiple AR5 climate models and concluded that the sensitivity of both inter-annual and intra-annual variability in wind speeds from AOGCMs to the greenhouse gas concentration and radiative forcing is small and disproportionate. Karnauskas et al[51] investigated large-scale changes in wind power across the globe and revealed that the changes across the northern mid-latitudes are robust responses over time in both high and low future emissions scenarios, whereas the Southern Hemisphere changes appear critically sensitive to each individual emissions scenario.

On this basis, we further analyzed the changes in wind power density across the entire and the north of China relative to the baseline period. The spatiotemporal variations in wind energy potential exhibit a similar behavior to those in near-surface wind speed, but the changes are larger. Significant differences between seasons are detected for wind power density. The changes in spatial distribution in spring and autumn are similar,

but, in winter and summer, they are opposite. In general, the wind power density is expected to increase by about 5% in winter in the major wind fields in China, while significant decreases (by about 6% on average) are projected for other seasons (ie, spring, summer and autumn). The larger amplitude of change is found in May (decrease) and winter months (increase). For the northeast region of China, the wind energy potential would increase over 6 months in the year, including cold months (ie, from November to February) and hot months (ie, July and August).

The high-resolution climate simulations are emphasized in this paper because of their abilities in reproducing more detailed local or regional climate information, which mainly affect wind speed and direction directly. The experimental methods can also be used to other parts of the globe. The results of this research are of great importance for understanding where and to what extent the wind energy can be utilized to contribute renewable energy system development in China in support of its long-term climate change mitigation commitment and developing targeted public policies and measures in the context of global warming.

ACKNOWLEDGEMENTS

This research was supported by the China National Key Research and Development Plan Project (2018YFE0196000, 2016YFA0601502 and 2016YFC0502800) , Fundamental Research Funds for the Central Universities (2017MS049) and Environmental Protection Public Welfare Scientific Research Project (201509010).

ORCID

Junhong Guo https://orcid.org/0000-0002-6066-0583

REFERENCES

1. Alexander LV, Allen SK, Bindoff NL, et al. Climate change 2013: the physical science basis, in contribution of working group I (WGI) to the fifth assessment report (AR5) of the intergovernmental panel on climate change (IPCC). *Computational Geometry*. 2013;18(2):95-123.
2. Pašičko R, Branković Č, Šimić Z. Assessment of climate change impacts on energy generation from renewable sources in Croatia. *Renew Energy*. 2012;46:224-231.
3. Carvalho D, Rocha A, Gómez-Gesteira M, Silva Santos C. Potential impacts of climate change on European wind energy resource under the CMIP5 future climate projections. *Renew Energy*. 2017;101:29-40.
4. Davy R, Gnatiuk N, Pettersson L, Bobylev L. Climate change impacts on wind energy potential in the European domain with a focus on the Black Sea. *Renewable & Sustainable Energy Reviews*. 2018;81:1652-1659.
5. China National Renewable Energy Center (CNREC). 2017. China Renewable Energy Outlook 2017.
6. Johnson DL, Erhardt RJ. Projected impacts of climate change on wind energy density in the United States. *Renew Energy*. 2016;85:66-73.
7. Tobin I, Vautard R, Balog I, et al. Assessing climate change impacts on European wind energy from ENSEMBLES high-resolution climate projections. *Clim Change*. 2015;128(1-2):99-112.
8. Wang J, Qin S, Zhou Q, Jiang H. Medium-term wind speeds forecasting utilizing hybrid models for three different sites in Xinjiang, China. *Renew Energy*. 2015;76:91-101.
9. Abolude A, Zhou W, Leung Y. Regional impact assessment of monsoon variability on wind power availability and optimization in Asia. *Atmos*. 2017;8(11):219
10. Mao Y, Monahan A. Predictive anisotropy of surface winds by linear statistical prediction. *J Climate*. 2017;30(16):6183-6201.
11. Shamshirband S, Mohammadi K, Tong CW, et al. RETRACTED ARTICLE: application of extreme learning machine for estimation of wind speed distribution. *Climate Dynam*. 2016;46(5-6):1893-1907.
12. Chang GW, Lu HJ, Chang YR, Lee YD. An improved neural network-based approach for short-term wind speed and power forecast. *Renew Energy*. 2017;105:301-311.
13. Ileană I, Muntean M, Rîşteiu M. Short term wind speed forecasting based on cluster analysis and ANN in wind farms. In: *Proc. SPIE 8411*, Advanced Topics in Optoelectronics, Microelectronics, and Nanotechnologies VI, 84110U (1 November 2012); https://doi.org/10.1117/12.966393
14. Niu T, Wang J, Zhang K, Du P. Multi-step-ahead wind speed forecasting based on optimal feature selection and a modified bat algorithm with the cognition strategy. *Renew Energy*. 2018;118:213-229.
15. Kulkarni S, Huang HP. Changes in surface wind speed over North America from CMIP5 model projections and implications for wind energy. *Advances in Meteorology*. 2014;2014:1-10.
16. Vautard R, Cattiaux J, Yiou P, Thépaut JN, Ciais P. Northern hemisphere atmospheric stilling partly attributed to an increase in surface roughness. *Nat Geosci*. 2010;3(11):756-761.
17. Wang X, Huang G, Lin Q, et al. A stepwise cluster analysis approach for downscaled climate projection - a Canadian case study. *Environ Model Software*. 2013;49(49):141-151.
18. Guo J, Huang G, Wang X, Li Y, Lin Q. Dynamically-downscaled projections of changes in temperature extremes over China. *Climate Dynam*. 2018;50(3-4):1045-1066.
19. Pryor SC, Barthelmie RJ. Climate change impacts on wind energy: a review. *Renewable & Sustainable Energy Reviews*. 2010;14(1):430-437.
20. Guo J, Huang G, Wang X, Li Y, Yang L. Future changes in precipitation extremes over China projected by a regional climate model ensemble. *Atmos Environ*. 2018;188:142-156.
21. Omrani H, Jourdier B, Beranger K, et al. Investigation on the offshore wind energy potential over the north western Mediterranean Sea in a regional climate system model[C]. *Renewable Energy Congress*. 2014;1-6.
22. Pryor SC, Barthelmie RJ, Kjellström E. Potential climate change impact on wind energy resources in northern Europe: analyses using a regional climate model. *Climate Dynam*. 2005;25(7-8):815-835.

23. Cantet P, Déqué M, Palany P, Maridet JL. The importance of using a high-resolution model to study the climate change on small islands: the Lesser Antilles case. *Tellus a: Dynamic Meteorology and Oceanography*. 2014;66(1):24065
24. Lee JW, Hong SY. Potential for added value to downscaled climate extremes over Korea by increased resolution of a regional climate model. *Theor Appl Climatol*. 2014;117(3-4):667-677.
25. Dosio A, Panitz H-J, Schubert-Frisius M, Lüthi D. Dynamical downscaling of cmip5 global circulation models over cordex-africa with cosmo-clm: evaluation over the present climate and analysis of the added value. *Climate Dynam*. 2015;44(9-10):2637-2661.
26. Xiong Z, Huang G, Wang X, Cheng G. Dynamically-downscaled temperature and precipitation changes over Saskatchewan using the precis model. *Climate Dynam*. 2018;50(3-4):1321-1334.
27. Mounkaila MS, Abiodun BJ, Omotosho JB. Assessing the capability of cordex models in simulating onset of rainfall in west africa. *Theoretical & Applied Climatology*. 2015;119(1-2):255-272.
28. Marengo JA, Jones R, Alves LM, Valverde MC. Future change of temperature and precipitation extremes in South America as derived from the precis regional climate modeling system. *Int J Climatol*. 2010;29(15):2241-2255.
29. Li Y, Wu X-P, Li Q-S, Tee KF. Assessment of onshore wind energy potential under different geographical climate conditions in China. *Energy*. 2018;152:498-511.
30. Wu J, Wang J, Chi D. Wind energy potential assessment for the site of Inner Mongolia in China. *Renew Sustain Energy Rev*. 2013;21:215-228.
31. Keyhani A, Ghasemi-Varnamkhasti M, Khanali M, Abbaszadeh R. An assessment of wind energy potential as a power generation source in the capital of Iran, Tehran. *Energy*. 2010;35(1):188-201.
32. Jiang Y, Luo Y, Zhao Z, Shi Y, Xu Y, Zhu J. Projections of wind changes for 21st century in China by three regional climate models. *Chin Geogr Sci*. 2010;20(3):226-235.
33. Wang X, Huang G, Liu J. Twenty-first century probabilistic projections of precipitation over Ontario, Canada through a regional climate model ensemble. *Climate Dynam*. 2016;46(11-12):3979-4001.
34. Jones RG, Noguer M, Hassell DC, et al. *Generating high resolution climate change scenarios using PRECIS*. Exeter, UK: Met Office Hadley Centre; 2004:40.
35. Gregory D, Rowntree PR. A mass flux convection scheme with representation of cloud ensemble characteristics and stability-dependent closure. *Mon Weather Rev*. 1990;118(7):1483-1506.
36. Gregory D, Kershaw R, Inness PM. Parametrization of momentum transport by convection II: tests in single column and general circulation models. *Q J Roy Meteorol Soc*. 1997;123(541):1153-1183.
37. Slingo A, Wilderspin RC. Development of a revised longwave radiation scheme for an atmospheric general circulation model. *Q J Roy Meteorol Soc*. 1986;112(472):371-386.
38. Slingo A. GCM parameterization for the shortwave radiative properties of water clouds. *J Atmos Sci*. 1989;46(10):1419-1427.
39. Berrisford P, Dee D, Poli P, et al. The ERA-interim archive: version 2.0. Nihon Seirigaku Zasshi. *Journal of the Physiological Society of Japan*. 2011;31(10):1-9.
40. Sun ZQ, Xiang J, Guan YP. Wind energy in the offshore areas of China based on ERA-interim reanalysis data. *Marine Forecasts*. 2016;33(3):50-56.
41. Wan Y, Zhang J, Meng J, Wang J. Exploitable wave energy assessment based on ERA-interim reanalysis data-a case study in the East China Sea and the South China Sea. *Acta Oceanologica Sinica*. 2015;34(9):143-155.
42. Song L, Liu Z, Wang F. Comparison of wind data from ERA-interim and buoys in the yellow and East China seas. *Chinese J Oceanol Limnol*. 2015;33(1):282-288.
43. Taylor KE. Summarizing multiple aspects of model performance in a single diagram. *J Geophys Res Atmos*. 2001;106(D7):7183-7192.
44. Hamed KH, Rao AR. A modified Mann-Kendall trend test for autocorrelated data. *J Hydrol*. 1998;204(1-4):182-196.
45. Ahmed SM. Assessment of irrigation system sustainability using the Theil–Sen estimator of slope of time series. *Sustainability Science*. 2014;9(3):293-302.
46. Bloom A, Kotroni V, Lagouvardos K. Climate change impact of wind energy availability in the eastern Mediterranean using the regional climate model PRECIS. *Natural Hazards & Earth System Sciences & Discussions*. 2008;8(6):1249-1257.
47. Fant C, Schlosser CA, Strzepek K. The impact of climate change on wind and solar resources in southern Africa. *Appl Energy*. 2016;161:556-564.
48. Mcelroy MB, Lu X, Nielsen CP, Wang Y. Potential for wind-generated electricity in China. *Science*. 2009;325(5946):1378-1380.
49. Ouyang W, Shi Y, Hao F, Jiao W. A comparison of general circulation models and their application to temperature change assessments in a high-latitude agricultural area in northeastern China. *Climate Dynam*. 2016;47(1-2):651-666.
50. Lu X, Mcelroy MB, Kiviluoma J. Global potential for wind-generated electricity. *Proc Natl Acad Sci U S a*. 2009;106(27):10933-10938.
51. Karnauskas KB, Lundquist JK, Zhang L. Southward shift of the global wind energy resource under high carbon dioxide emissions. *Nat Geosci*. 2017;11(1):38
52. Guo H, Xu M, Hu Q. Changes in near-surface wind speed in China: 1969–2005. *Int J Climatol*. 2011;31(3):349-358.
53. Chen L, Pryor SC, Li D. Assessing the performance of intergovernmental panel on climate change AR5 climate models in simulating and projecting wind speeds over China. *J Geophys Res Atmos*. 2012;117(D24):

SUPPORTING INFORMATION

Additional supporting information may be found online in the Supporting Information section at the end of this article.

How to cite this article: Guo J, Huang G, Wang X, Xu Y, Li Y. Projected changes in wind speed and its energy potential in China using a high-resolution regional climate model. *Wind Energy*. 2019;1–15. https://doi.org/10.1002/we.2417